Latitudinal distribution of the deuterium to hydrogen ratio in the atmospheric water vapor retrieved from IMG/ADEOS data

Vyacheslav I. Zakharov,[1] Ryoichi Imasu,[2] Konstantin G. Gribanov,[1] Georg Hoffmann,[3] and Jean Jouzel[3]

Received 7 January 2004; revised 12 March 2004; accepted 13 May 2004; published 19 June 2004.

[1] Latitudinal distribution of the columnar deuterium/hydrogen ratio of atmospheric water vapor, δD_{vap}, was retrieved from high-resolution infrared spectra. Interferometric Monitor for Greenhouse gases (IMG) sensor aboard the ADvanced Earth Observing Satellite (ADEOS) observed the spectra over the ocean during the operational period from December 1996 through June 1997. The latitudinal mean δD_{vap} was relatively large with values around −100‰ in the tropical region decreasing down to minimal values of −800‰ at high latitudes. For retrieving δD_{vap}, a type of spectral fitting method was adopted using a forward/retrieval calculation code developed by *Gribanov et al.* [2001]. This method is expected to be applicable for data analyses of future satellite sensors such as IASI and TES. *INDEX TERMS:* 1040 Geochemistry: Isotopic composition/chemistry; 1655 Global Change: Water cycles (1836); 1836 Hydrology: Hydrologic budget (1655); 3360 Meteorology and Atmospheric Dynamics: Remote sensing; 3394 Meteorology and Atmospheric Dynamics: Instruments and techniques. **Citation:** Zakharov, V. I., R. Imasu, K. G. Gribanov, G. Hoffmann, and J. Jouzel (2004), Latitudinal distribution of the deuterium to hydrogen ratio in the atmospheric water vapor retrieved from IMG/ADEOS data, *Geophys. Res. Lett.*, *31*, L12104, doi:10.1029/2004GL019433.

1. Introduction

[2] Isotopic composition of atmospheric water provides important insight into water circulation and water's origin because isotopomer ratios of water (HDO/H_2O, $H_2{}^{18}O/H_2O$) are affected strongly by water evaporation conditions and condensation history during the air mass transport.

[3] Previous studies have mostly measured isotopic data from rainwater at ground stations to elucidate how local climate conditions influence the isotopic signal in rain water [e.g., *Rozanski et al.*, 1993]. Water circulation has been investigated on various meteorological scales using isotopic data from rainfall: the mesoscale, synoptic scale, and continental scale [*Araguas-Araguas et al.*, 1998; *Federer et al.*, 1982; *Gat et al.*, 1994; *Gedzelman et al.*, 1989; *Lawrence and Gedzelman*, 1996]. Notwithstanding, few studies have addressed water vapor based on in situ measurements [*Ehhalt*, 1974; *Taylor*, 1972; *He and Smith*, 1999; *White and Gedzelman*, 1984] because of the difficult sampling procedure. That procedure must protect the isotopic ratio of water vapor from alteration by the measuring process.

[4] Isotopic water vapor data are also useful for validating Atmospheric General Circulation Models (AGCMs). Numerous AGCMs have been fitted with water isotope diagnostics and the comparison between simulated and observed isotope signals bear a big potential for improving transport and cloud parameterizations processes. These "isotopic models" have been used to discuss water circulation, water budget, and further water recycling processes [*Jouzel et al.*, 1991; *Koster et al.*, 1992, 1993; *Hoffmann et al.*, 1998].

[5] Some attempts have been made to measure isotopic composition using remote sensing techniques, mostly limb sounding, for elucidating stratospheric water circulation [*Abbas et al.*, 1987; *Dinelli et al.*, 1997; *Irion et al.*, 1996; *Johnson et al.*, 2001]. Nevertheless, they have not been applied to the tropospheric measurements because clouds can contaminate limb sounding data easily.

[6] This study presents, for the first time, latitudinal distribution of deuterium/hydrogen ratio of water vapor (δD_{vap}) derived from infrared radiation spectra measured by Interferometric Monitor for Greenhouse gases (IMG) sensor [*Imasu*, 1999] aboard the ADvanced Earth Observing Satellite (ADEOS).

2. IMG Data and Retrieval Technique

[7] IMG was a Fourier transform type spectrometer in operation from November 1996 through June 1997. More than 130,000 terrestrial thermal radiation spectra were measured during its operational period [*Imasu*, 1999]. The spectrum range and resolution were 650–2500 cm^{-1} and 0.1 cm^{-1} (after apodization), respectively.

[8] This study used only clear sky data for analysis. Cloud screening was made based on the IMG data itself and visible imagery observed by the Ocean Color Temperature Scanner (OCTS) aboard ADEOS. The data area was restricted only over ocean within 70°N–70°S and 130°W–160°W because the ocean surface emissivity closely resembles that of black body. Uncertainty of retrieval that is attributable to unknown variations of surface emissivity is negligible in this case.

[9] The modified version of Fine InfraRed Explorer for Atmospheric Radiation MeasurementS (FIRE–ARMS) software package [*Gribanov et al.*, 2001] (see http://remotesensing.ru) was used both for simulation of spectra observed by IMG and for the retrieval of atmospheric parameters.

[10] The retrieval procedure can be subdivided into three steps [*Zakharov et al.*, 2002]. The first step is the retrieval of

[1]Global Ecology and Remote Sensing Laboratory, Department of Physics, Ural State University, Ekaterinburg, Russia.
[2]Center for Climate System Research, University of Tokyo, Tokyo, Japan.
[3]Institut Pierre Simon Laplace Laboratoire des Sciences du Climat et de l'Environnement, UMR CEA-CNRS 1572 CE Saclay, Gif sur Yvette, France.

0094-8276/04/2004GL019433

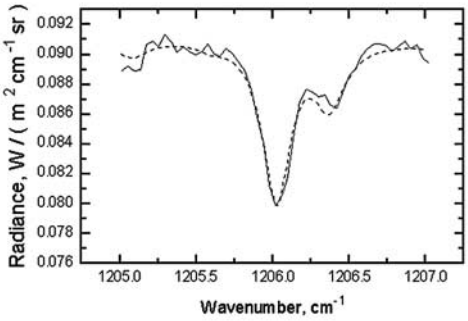

Figure 1. Radiance spectra around an absorption line of HDO. Solid and dashed lines represent the spectra measured by IMG sensor and synthesized for retrieved HDO to H_2O ratios, respectively [*Zakharov et al.*, 2002].

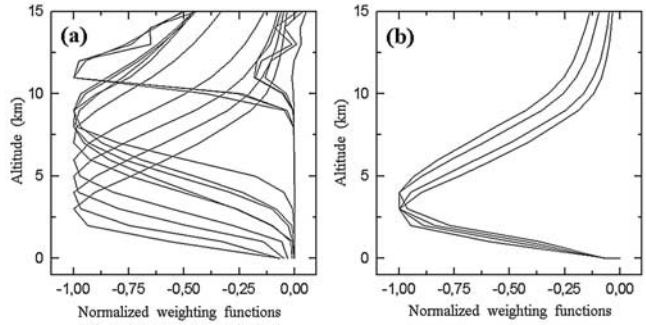

Figure 2. Normalized weighting functions of the spectral channels used for (a) H_2O and (b) HDO retrievals.

a temperature profile from IMG observation using a set of non-overlapping spectral intervals in the range of 675–825 cm^{-1}. Second is retrieval of water vapor (main isotopomer). The spectral interval of 1197–1200 cm^{-1} was used for H_2O profile retrieval and a total column amount of H_2O calculation. The third step is retrieval of the HDO column amount and then the D/H ratio. HDO effective profile retrieval and its column amount were made using a 1205–1207 cm^{-1} spectral interval. The effective profile is that which provides good adjustment of observed and simulated spectra in the given spectral interval. These procedures were carried out sequentially. The model vertical distribution of HDO presented by *Rozanski and Sonntag* [1982] was used as a first-guess profile.

[11] Retrieval algorithms built into the FIRE-ARMS determine the minimum of an objective function defined as

$$F = \sum_{i=1}^{M} \left[\frac{W_i^{obs}}{W_i^{calc}} - \frac{W_i^{calc}}{W_i^{obs}} \right]^2, W_i^{calc} \equiv W^{calc}(T, P, n_\alpha, \nu_i)|_{h=H}, \quad (1)$$

where W_i^{obs} and W_i^{calc} are observed and calculated radiances, respectively, at the ith spectral frequency. Adjustable parameters T, P, n_α are vectors of temperature, pressure and αth constituent concentrations at nodes of height mesh. Variable M is the number of spectral channels. *Gribanov et al.* [2001] described details of this method.

[12] All spectral calculations are first performed at high spectral resolution (line-by-line) using spectral parameters from HITRAN-96 database [*Rothman et al.*, 1998]. They are then convoluted with instrumental line shape function of the IMG. A water vapor continuum model was taken from [*Clough et al.*, 1989]; aerosol models recommended by *Deepak and Gerber* [1983] were used. Sea surface temperatures (SST) were computed from ocean emissivity based on the HITRAN-96 database.

[13] Isotope geochemists usually define δD as [*Craig*, 1961]:

$$\delta D = \left(\frac{(D/H)}{(D/H)_{SMOW}} - 1 \right) \times 1000, \quad (2)$$

Therein, *SMOW* stands for Standard Mean Ocean Water.

3. Results on Determination of δD_{vap} Latitudinal Distribution From IMG Data

[14] An example of a radiance spectrum around the absorption line of HDO is shown in Figure 1. Solid and dashed lines represent the spectra measured by IMG and synthesized for retrieved HDO to H_2O ratios, respectively.

[15] Normalized weighting functions of the spectral channels used for water vapor and HDO retrieval are shown in Figure 2. Apparently, the weighting function peaks of HDO are located in 3–5 km height and most information from IMG spectra on HDO concentration comes from the middle troposphere.

[16] Our formerly described retrieval method was applied to data analysis of IMG spectra. According to test calculations, errors of retrieved temperature profiles are not greater than 0.2 K for surface temperature and are not greater than 1 K for tropospheric layers. The errors for H_2O profile retrieval are not greater than 10% for the troposphere [*Gribanov et al.*, 2003]. Corresponding errors for columnar amounts of the water vapor isotopomers are even less, 1%–2%, because the profile error is generally random and can be reduced by vertical averaging. The accuracy of δD_{vap} depends only on errors in determination of columnar amounts of H_2O and HDO. The last is about 20‰ for the tropics and increases to 170‰ at high latitudes because the signal-to-noise ratio of IMG spectra decreases in cold atmospheres.

[17] Horizontal distribution of the retrieved δD_{vap} is shown in Figure 3 (left) together with the zonal mean computed in 3° latitudinal steps (right). Error bars show the standard deviation of the data in each 3° latitudinal step; open circles represent that only one datum was retrieved in the step. δD_{vap} is relatively high in the tropics with values at about −100‰. It decreases gradually toward middle latitudes. At high latitudes, the values are scattered widely; the minimum value is about −800‰. Weak seasonal variation, particularly in the location of the maximum of δD_{vap}, can be seen in the same type of figures drawn for each month. However, they are not presented in this paper because the number of IMG data selected was not sufficient to compute a statistically robust seasonal cycle.

[18] To examine the degree of influence of the initial fractionation process occurring at the sea surface, each δD_{vap} value was plotted as a function of SST at which IMG data were observed in Figure 4. The SST data were obtained from the National Environmental Satellite Data and Information Service (NESDIS) data archive. Colors of respective plot points represent the latitudinal zones of the data. The solid line in the figure shows the temperature

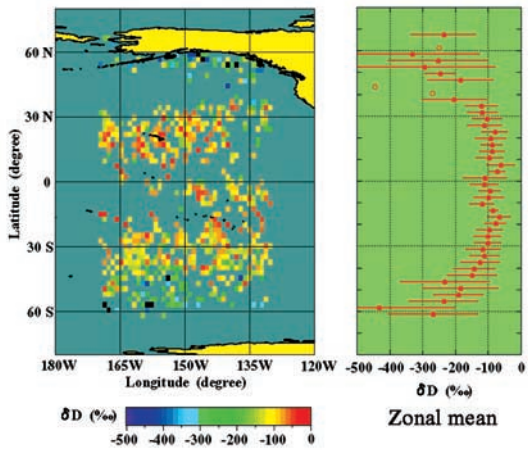

Figure 3. Horizontal distribution of retrieved δD_{vap} values (left) and the zonal mean in 3° latitudinal steps (right). Error bars show the standard deviation of the data in each 3° latitudinal step and open circles represent that only one datum was retrieved in the step. Only the clear sky condition data observed during the IMG observational period from December 1996 to June 1997 were used for analysis.

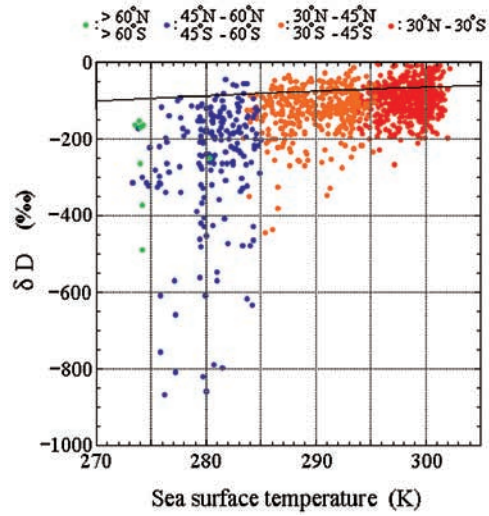

Figure 4. Relationship between retrieved δD_{vap} values and sea surface temperature at which the IMG data were observed. The solid line represents the temperature dependency of δD_{vap} calculated for a simple two-phase (vapor/liquid) distillation model.

dependency of δD_{vap} calculated with a formula presented by *Merlivat and Nief* [1967], as

$$\delta D_{vap} = (1/\alpha - 1.0) \times 1000,$$
$$\ln \alpha = 15013.0/T^2 - 10.00 \times 10^{-2}, \quad (3)$$

where T and α are temperature and the equilibrium fractionation coefficient, respectively. This formula was derived empirically from laboratory experiments based on a simple two-phase (vapor/liquid) distillation approach. Although the model is an oversimplification compared to the real processes influencing the isotopic composition of tropospheric water vapor, its use here is intended only as a reference point for comparison with the retrieved δD_{vap} signal.

4. Discussion

[19] The main sources of uncertainties in the retrieval scheme in this study are aerosols, IMG measurement noise, and first-guess profiles of HDO. We used the standard maritime WMO aerosol model [*Deepak and Gerber*, 1983], but more realistic spectral dependency of extinction coefficient and vertical distribution profiles of aerosols for each IMG observation point are required for more precise retrieval of temperature and atmospheric constituent profiles. Measurement noise is a main source of uncertainty at high latitudes, where radiance of the cold atmosphere is weak. Lower noise, which is anticipated with future sensors, will engender better accuracy of δD determination, especially at high latitudes. In addition, a better model for vertical profile of HDO may improve the retrieval of δD.

[20] Although δD_{vap} values scattered mainly because of the signal noise, it can be said the latitudinal gradient of δD_{vap} shown in Figure 4 actually existed. Latitudinal distribution (or SST dependency) of δD_{vap} can be explained as a composite of isotopic fractionation effects and air mass transport effect.

[21] For a first evaluation of the retrieved δD_{vap} values we added an empirically derived δD_{vap}-temperature curve in Figure 4. The formula used for the calculation has been derived under a simple two-phase distillation condition [*Merlivat and Nief*, 1967]. Moreover, it can be applicable for evaporation of water vapor from the sea surface assuming that: (1) water vapor has been formed in equilibrium with SSTs; and that (2) condensation formed from the cooling vapor mass is extracted immediately from the system ("open system").

[22] If condensation of water vapor occurs, or if air with strongly depleted water vapor is advected, δD_{vap} can be smaller than that expected from such a two-phase distillation model controlled only by the corresponding SST. Figure 4 that the maximum δD_{vap} values exists close to the δD_{vap}–temperature curve in middle latitudes, but with a large scatter. However, some satellite-derived values markedly exceed the model values in the tropics. This fact suggests the possibility of kinetic fractionation or evaporative enrichment of rain droplets below the cloud base.

[23] When air masses are transported from the tropics, they typically undergo successive isotopic depletion by a continuous condensation process. Synchronously, δD values of precipitation and vapor become increasingly depleted when vapor recharge becomes less effective because of lower SSTs. The δD_{vap} values widely scatter depending on the cloud temperature and depth of cloud convection. These processes can explain smaller δD_{vap} values observed in middle or high latitude regions.

[24] For the future, we are mostly interested in the origin of water vapor observed at each place concerned. Generally, the d-excess value, which is defined as the $\delta^{18}O$ value at the intercept of a δD vs. $\delta^{18}O$ plot, is used to discuss the water vapor origin [*Armengaud et al.*, 1998; *Ciais and Jouzel*, 1994]. It is principally possible to derive a d-excess value from IMG spectrum data. However, we must reduce noise

levels of the IMG data for such an approach by adopting some additional effective data processing method to obtain realistic d-excess data.

5. Conclusion

[25] Latitudinal distribution of columnar deuterium/hydrogen ratio δD_{vap} of the atmospheric water vapor has been retrieved from high resolution infrared spectra observed over the ocean by IMG/ADEOS sensor using a forward/retrieval code. It is named FIRE-ARMS. Results showed that δD_{vap} were in the tropics in the order of about −100‰. From such comparable enriched values, we infer that isotope signals decrease gradually toward middle latitudes and eventually reach extremely low values of around −800‰ at high latitudes.

[26] The reason for the latitudinal distribution feature of δD_{vap} was described considering the two-phase distillation process starting at the sea water surface, D/H separation through water vapor condensation in clouds, and air mass transport from tropical regions to high latitudes. Comparison with a simple first-order isotope model corroborates results of our retrieval technique. Further studies will extend such a comparison using more detailed spatial and temporal information from AGCMs fitted with water isotope diagnostics [*Hoffmann et al.*, 1998]. Moreover, this study calls for in situ measurements of δD_{vap} in the marine boundary layer, which could validate our analysis. We emphasized the importance of d-excess values for discussing the origin of water vapor and argued for capability of deriving d-excess from IMG data.

[27] The data analysis method adopted in this study has no specific restriction to the same type of analysis of thermal infrared spectra as IMG data. For that reason, we expect that this method is applicable for data analysis of future satellite sensors such as the Infrared Atmospheric Sounding Interferometer (IASI) [*Lerner et al.*, 2002] and the Tropospheric Emission Spectrometer (TES) [*Luo et al.*, 2002].

[28] **Acknowledgments.** This study was partially supported by Japan Science and Technology Corporation (JST) and Global Environment Research Fund (GERF) of Ministry of the Environment (ME) of Japan. We gratefully acknowledge Dr. Tadao Aoki, Dr. F. M. Breon, and Prof. Atsuko Sugimoto for advising us on problems of monitoring atmospheric deuterium and contributing helpful discussions and comments on the results.

References

Abbas, M. M., et al. (1987), Stratospheric O_3, H_2O, and HDO distributions from balloon-based far-infrared observations, *J. Geophys. Res.*, *92*, 8354–8364.

Araguas-Araguas, L., K. Froehlich, and K. Rozanski (1998), Stable isotope composition of precipitation over southeast Asia, *J. Geophys. Res.*, *103*, 28,721–28,742.

Armengaud, A., R. D. Koster, J. Jouzel, and P. Ciais (1998), Deuterium excess in Greeland snow: Analysis with simple and complex models, *J. Geophys. Res.*, *103*, 8653–8947.

Ciais, P., and J. Jouzel (1994), Deuterium and oxygen-18 in precipitation: Isotopic model, including mixed cloud processes, *J. Geophys. Res.*, *99*, 16,793–16,803.

Clough, S. A., et al. (1989), Line shape and the water vapor continuum, *Atmos. Res.*, *23*, 229–241.

Craig, H. (1961), Standards for reporting concentrations of deuterium and oxygen-18 in natural water, *Science*, *133*, 1833–1834.

Deepak, A., and H. E. Gerber (Eds.) (1983), *Report of the Experts Meeting on Aerosols and their Climatic Effects*, World Meteorol. Org., Geneva.

Dinelli, B. M., et al. (1997), Measurement of the isotopic ratio distribution of $HD^{16}O$ and $H_2{}^{16}O$ in the 20–38 km altitude range from far-infrared spectra, *Geophys. Res. Lett.*, *24*, 2003–2006.

Ehhalt, D. H. (1974), Vertical profiles of HTO, HDO and H_2O in the troposphere, *NCAR Tech. Note NCAR-TN/STR-100*, Natl. Cent. for Atmos. Res., Boulder, Colo.

Federer, B., et al. (1982), Stable isotopes in hailstones 1—The isotopic cloud model, *J. Atmos. Sci.*, *39*, 1323–1335.

Gat, J. R., C. J. Bowser, and C. Kendall (1994), The contribution of evaporation from the Great Lakes to the continental atmosphere: Estimate based on stable isotope data, *Geophys. Res. Lett.*, *21*, 557–560.

Gedzelman, S. D., et al. (1989), The megalopolitan snowstorm of 11–12 February 1983—Isotopic composition of the snow, *J. Atmos. Sci.*, *46*, 1637–1649.

Gribanov, K. G., et al. (2001), A new software tool for radiative transfer calculations and its application to IMG/ADEOS data, *J. Quant. Spectrosc. Radiat. Transfer*, *68*, 435–451.

Gribanov, K. G., et al. (2003), Retrieval of temperature and humidity profiles from the Earth's IR spectra based on singular decomposition of covariance matrices, *Atmos. Oceanic Opt.*, *16*, 530–535.

He, H., and R. B. Smith (1999), Stable isotope composition of water vapor in the atmospheric boundary layer above the forests of New England, *J. Geophys. Res.*, *104*, 11,657–11,673.

Hoffmann, G., M. Werner, and M. Heimann (1998), Water isotope module of the ECHAM atmospheric general circulation model: A study on timescales from days to several years, *J. Geophys. Res.*, *103*, 16,871–16,896.

Imasu, R. (1999), Meridional distribution feature of minor constituents as observed by IMG Sensor aboard ADEOS satellite, *Adv. Space Res.*, *25*, 959–962.

Irion, F. W., et al. (1996), Stratospheric observations of CH_3D and HDO from ATMOS infrared solar spectra: Enrichments of deuterium in methane and implications for HD, *Geophys. Res. Lett.*, *23*, 2381–2384.

Johnson, D. G., K. W. Jucks, W. A. Traub, and K. V. Chance (2001), Isotopic composition of stratospheric water vapor: Measurements and photochemistry, *J. Geophys. Res.*, *106*, 12,211–12,217.

Jouzel, J., G. L. Russell, J. W. C. White, and W. S. Broecker (1991), Simulations of the HDO and $H_2{}^{18}O$ atmospheric cycles using the NASA GISS general-circulation model-sensitivity experiments for present-day conditions, *J. Geophys. Res.*, *96*, 7495–7507.

Koster, R. D., et al. (1992), Origin of July Antarctic precipitation and its influence on deuterium content: A GCM analysis, *Clim. Dyn.*, *7*, 195–203.

Koster, R. D., D. Perry de Valpine, and J. Jouzel (1993), Continental water recycling and $H_2^{18}O$ concentrations, *Geophys. Res. Lett.*, *20*, 2215–2218.

Lawrence, J. R., and S. D. Gedzelman (1996), Low stable isotope ratios of tropical cyclone rains, *Geophys. Res. Lett.*, *23*, 527–530.

Lerner, J. A., E. Weisz, and G. Kirchengast (2002), Temperature and humidity retrieval from simulated Infrared Atmospheric Sounding Interferometer (IASI) measurements, *J. Geophys. Res.*, *107*(D14), 4189, doi:10.1029/2001JD900254.

Luo, M., R. Beer, D. J. Jacob, J. A. Logan, and C. D. Rodgers (2002), Simulated observation of tropospheric ozone and CO with the Tropospheric Emission Spectrometer (TES) satellite instrument, *J. Geophys. Res.*, *107*(D15), 4270, doi:10.1029/2001JD000804.

Merlivat, L., and G. Nief (1967), Fractionnement isotopique lors des changements d'etat solide-vapeur et liquide-vapeur de l'eau a des temperatures inferieures a 0°C, *Tellus*, *1*, 122–127.

Rothman, L. S., et al. (1998), The HITRAN molecular spectroscopic database and HAWKS (HITRAN Atmospheric Workstation), *J. Quant. Spectrosc. Radiat. Transfer*, *60*, 665–710.

Rozanski, K., and C. Sonntag (1982), Vertical distribution of deuterium in atmospheric water vapour, *Tellus*, *34*, 135–141.

Rozanski, K., et al. (1993), Isotopic patterns in modern global precipitation, in *Climate Change in Continental Isotopic Records*, *Geophys. Monogr. Ser.*, vol. 78, edited by P. K. Swart et al., pp. 1–37, AGU, Washington, D. C.

Taylor, C. B. (1972), The vertical distribution of the isotopic concentrations of tropospheric water vapour over continental Europe and their relationship to tropospheric structure, *N. Z. Inst. Nucl. Sci. Rep. INS-R-107*.

White, J. W. C., and S. D. Gedzelman (1984), The isotopic composition of atmospheric water-vapor and the concurrent meteorological conditions, *J. Geophys. Res.*, *89*, 4937–4939.

Zakharov, V. I., et al. (2002), D/H latitudinal distribution in atmosphere retrieved from IMG spectra, *Proc. SPIE Int. Soc. Opt. Eng.*, *4897*, 65–71.

K. G. Gribanov and V. I. Zakharov, Global Ecology and Remote Sensing Laboratory, Department of Physics, Ural State University, 51 Lenin Ave., Ekaterinburg 620083, Russia.

G. Hoffmann and J. Jouzel, IPSL/Laboratoire des Sciences du Climat et de l'Environnement, UMR CEA-CNRS 1572 CE Saclay, Orme des Merisiers, F-91191 Gif sur Yvette, France.

R. Imasu, Center for Climate System Research, University of Tokyo, 4-6-1 Komaba, Meguro-ku Tokyo 153-8904, Japan. (imasu@ccrs.u-tokyo.ac.jp)